Short Communication

Influence of Hypophosphite on Efficiency and Coating Qualities of Electroless Ni-P Deposits on Magnesium Alloy AZ91D

Ruixue Sun[1], Gang Yu[1,*], Zhihui Xie[1], Bonian Hu[1,2,*], Jun Zhang[1], Xiaomei He[2], Xueyuan Zhang[1,*]

[1] State Key Laboratory of Chemo/Biosensing and Chemometrics, College of Chemistry and Chemical Engineering, Hunan University, Changsha 410082, P. R. China
[2] Department of Materials and Chemical Engineering, Hunan Institute of Technology, Hengyang 421002, P. R. China
[*]E-mail: yuganghnu@163.com; hbonain@163.com; xzhan94@163.com

The effect of reducing agent (sodium hypophosphite) on plating rate, reduction efficiency of sodium hypophosphite, properties of baths and coatings in electroless Ni-P plating on magnesium alloys were studied. The results showed that the concentration of sodium hypophosphite in the bath had impact on properties of bath and coatings. Low concentration of sodium hypophosphite would reduce the reactivity of the bath and form incompact coatings with poor corrosion resistance. Exorbitant concentration of sodium hypophosphite would lower reduction efficiency and efficiency of nickel deposition in electroless Ni-P plating process and coatings adhesion. The specific phosphorus content of coatings with high corrosion resistance was obtained by controlling the concentration of sodium hypophosphite. High stability of bath was established based on high reduction efficiency and efficiency of nickel deposition. The effect of concentration of sodium hypophosphite provided a route for controlling properties of coatings and monitoring bath stability. When the concentration of sodium hypophosphite in the bath was controlled to 25-30 g·dm^{-3}, the compact Ni-P coatings with strong adhesion and good corrosion resistance were obtained and the electroless bath possessed high stability.

1. INTRODUCTION

Magnesium alloys are widely employed in aerospace, automobile, electronic devices and other fields owing to their low density, high strength-to-weight ratio, high damping, good castability and machinability. Nevertheless, easy corrosion, high chemical reactivity and abrasion resistance of magnesium alloy limit their development and applications [1, 2]. So far, all magnesium alloys must

choose appropriate method of surface treatment in order to improve their properties before applied [3]. Electroplating, anodizing film, surface modification, organic coatings and metal coatings are common methods of surface treatment. Various types of coatings can be applied to increase corrosion resistance, but electroless nickel (EN) coatings are superior. EN coatings show their excellent performance increasingly mainly owing to the advantages such as wear and corrosion resistance, adaptability for uniform coatings on complex shapes [4-5].

EN coatings are produced by using reducing agent to make nickel ions deposited on the magnesium substrate. Four reducing agents of sodium hypophosphite, sodium borohydride, dimethylamine borane, hydrazine are used in the chemical reduction of nickel ions from aqueous solutions. They are structurally similar in that each contains two or more reactive hydrogens, and nickel reduction is said to result from the catalytic dehydrogenation of the reducing agent [6]. The Ni-P alloy coatings obtained from bath using sodium hypophosphite as reducing agent have been widely used in electronics, machinery, automobile, aerospace, and valve industries because of their high hardness, coatings uniformity, as well as high wear and corrosion resistance [7].

The electroless Ni-P plating processes are very complex due to their special selfcatalyzed chemical reactions. Most investigations have been done concerning influences of bath condition on composition, microstructure, and functional properties of Ni-P alloys [8-10]. But they do not give much insight into reduction efficiency and efficiency of nickel deposition [11]. However, the full reduction efficiency and entire efficiency of nickel deposition in the plating bath is impossible due to the side reactions. The limited life span of bath makes the operation costs and bath disposal costs significantly higher. The reduction efficiency and efficiency of nickel deposition are important specifications for measuring bath properties. The higher reduction efficiency and efficiency of nickel deposition, the higher the bath stability it is. Thus it can avoid massive emissions of harmful ions in the bath, protect the environment and conserve resources.

There are many influence factors in electroless Ni-P plating, such as pretreatment which have important impact on coatings properties, bath composition and operation conditions. In this paper, we focused on effect of hypophosphite in the plating bath because of the high sensitivity to the bath life span and the qualities of coatings. Hence, the effect of hypophosphite on coatings qualities and bath properties were discussed in detail. It was a key to improve the efficiencies for reduction of hypophosphite and nickel deposition in order to control the coatings qualities and bath life.

2. EXPERIMENT

2.1 Experimental material

The specimens were made of AZ91D magnesium alloys in the form of plates 30 mm × 20 mm × 4 mm, whose chemical compositions are 8.77 wt.% Al, 0.74 wt.% Zn, 0.18 wt.% Mn, 0.001 wt.% Ni, 0.001 wt.% Fe and the remainder Mg.

2.2 The process of EN plating

The flows of electroless nickel (EN) plating were carried out with the following processes: ultrasonic cleaning, chemical degreasing, alkaline cleaning, acid cleaning, two activations and EN plating, as shown in Table 1.

Table 1. The process flow of EN plating

Process	Solution composition		Operation condition
Alkaline cleaning	NaOH	50 g·dm^{-3}	333 K
	Na$_3$PO$_4$·12H$_2$O	10 g·dm^{-3}	10 min
Acid pickling	HNO$_3$(68%)	30 g·dm^{-3}	Room temperature
	H$_3$PO$_4$(85%)	605 cm^3·dm^{-3}	30-40 s
Activation 1	K$_4$P$_2$O$_7$	120~200 g·dm^{-3}	
	Na$_2$CO$_3$	10~30 g·dm^{-3}	343±5 K
	KF·2H$_2$O	11 g·dm^{-3}	2-3 min
Activation 2	NH$_4$HF$_2$	95 g·dm^{-3}	Room temperature
	H$_3$PO$_4$	180 g·dm^{-3}	2-3 min
EN plating	NiSO$_4$·6H$_2$O	20 g·dm^{-3}	
	HF(40%)	12 cm^3·dm^{-3}	
	C$_6$H$_8$O$_7$·H$_2$O	5 g·dm^{-3}	pH : 5
	NH$_4$HF$_2$	10 g·dm^{-3}	358 K
	NH$_3$·H$_2$O(25%)	30 cm^3·dm^{-3}	60 min
	NaH$_2$PO$_2$·H$_2$O	5-40 g·dm^{-3}	
	H$_2$NCSNH$_2$	1 mg·dm^{-3}	
	pH adjustment	15-20 g·dm^{-3}	

2.3 Determination of the performances of bath and coatings

(1) Plating rate

The plating rate (v, μm·h^{-1}) was determined by weigh-plate-weigh method and expressed in the terms of the weight gain during the deposition process and can be calculated according to the following formula [12]:

$$v = \frac{\Delta m}{\rho \times S \times t} \times 10^4 \left(\mu m \cdot h^{-1} \right) \tag{1}$$

where Δm is the mass increment of the specimen before and after plating . S is the surface area of specimen, cm^2. ρ (the average density of the Ni-P deposit), g·cm^{-3}, is dependent on phosphorus content of coatings. t is the plating duration, h.

(2) Efficiency of nickel deposition

Nickel deposition efficiency (b) which is also called bath stability in the literature [13] is defined as follows:

$$b = \frac{\Delta m \times \text{Ni\%}}{\left(c_{0,\text{Ni}^{2+}} V_0 - c_{t,\text{Ni}^{2+}} V_t \right) M_{\text{Ni}}} \times 100\% \qquad (2)$$

Where Δm is the mass increment of the specimen before and after plating. Ni % stands for the Ni content (wt.%) in coatings. M_{Ni} (g·mol^{-1}), the molar mass of nickel. V_t (dm^3), the volume of plating solution after plating and V_0 (dm^3), the volume of plating solution before plating. $c_{0,\text{Ni}}$ and $c_{t,\text{Ni}}$ (mol·dm^{-3}) are the concentration of the nickel ions before and after plating, respectively.

(3) Reducing efficiency

The reducing efficiency (e_{SH}) is determined and calculated according to the following formula [14]:

$$e_{\text{SH}} = \frac{\dfrac{\Delta m \times (1 - \text{P\%})}{M_{\text{Ni}}} + 1.5 \dfrac{\Delta m \times \text{P\%}}{M_{\text{P}}}}{c_{0,\text{P}} V_0 - c_{t,\text{P}} V_t} \times 100\% \qquad (3)$$

Where Δm is the mass increment of the specimen before and after plating. P% is the phosphorus content (wt.%) in coatings. M_{Ni} (g·mol^{-1}) is the molar mass of nickel. M_{P} (g·mol^{-1}) is the molar mass of phosphorus. V_t (dm^3) is the volume of plating solution after plating and V_0 (dm^3) is the volume of plating solution before plating. $c_{0,\text{P}}$ and $c_{t,\text{P}}$ (mol·dm^{-3}) are the concentration of the sodium hypophosphite before and after plating, respectively.

(4) Coverage and adhesion of coatings

(a) Coatings coverage

The corrosion points unit area on the coatings by immersing specimens in 3.5 wt.% NaCl solution for 2 h was measured to evaluate coatings coverage [15].

(b) Coatings adhesion

Evaluation of adhesion was conducted to the following criteria at timings of direct after the plating and directly after 423 K of 1 h, wherein a state of swell occurrence on a plating surface or a state of peeling-off occurrence was observed on respective samples. The plating adhesion is classified into three grades. "×" stands for very poor adhesion and plating continuously sloughed-off. "△"indicates sometimes small plating swell occurs but no peeling off. "○" represents good qualities plating without swell and peel off [16].

(5) Corrosion resistance of Coatings

(a) Polarization curves

Polarization experiment was conducted in an electrolyte cell system with electrochemical work station (Interface 1000, Gamry Co., USA). Coatings polarization experiment was conducted in 3.5 wt.% NaCl solution at room temperature with a scanning rate of 1 mV·s^{-1}. Ni-P coatings were used as working electrodes. A platinum electrode and saturated calomel electrode (SCE) were used as counter and reference electrode, respectively.

(b) Neutral salt spray（NSS）

NSS test was conducted in 5 wt.% NaCl solution at 35±2 °C for 96 h based on ISO 3768-1976 [17].

(6) Characterization of surface morphology

Surface morphologies and compositions of were measured by scanning electron microscopy (SEM), a Hitachi-S4800 (Japan) matching with an energy dispersive X-ray (EDX) microanalysis system.

3. RESULTS AND DISCUSSION

3.1 EN plating reaction mechanism and plating rate equation

3.1.1 EN plating reaction mechanism analysis

In general, the overall reaction in an EN plating solution containing sodium hypophosphite as the reducing agent can be expressed as follows [18]:

$$NiL_m^{2+} + 4H_2PO_2^- + H_2O \rightarrow Ni + P + 3H_2PO_3^- + H^+ + \tfrac{3}{2}H_2 \uparrow + mL \qquad (4)$$
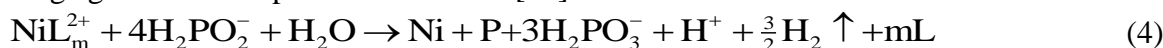
Based on electrochemical principle, electroless deposition is carried out through anodic and cathodic reactions. When EN plating is conducted by hypophosphite as reducing agent, anodic process is the oxidation of reducer "hypophosphite" with water and generated electrons. The electrons are used in the coupled cathodic processes for Ni-P plating and production of hydrogen gas [19]. This process can be represented as follows:

Anodic reaction:

$$H_2PO_2^- + H_2O \rightarrow H_2PO_3^- + 2H^+ + 2e^- \qquad (5)$$

Cathodic reaction:

$$NiL_m^{2+} + 2e^- \rightarrow Ni + mL \qquad (6)$$

$$2H^+ + 2e^- \rightarrow H_2 \qquad (7)$$

$$H_2PO_2^- + 2H^+ + e^- \rightarrow P + 2H_2O \qquad (8)$$
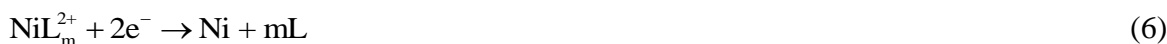
Hypophosphite participates in both the anodic reaction and the cathodic reactions according to Reaction (5) and (8).

Reaction (5) and (6) are combined:

$$H_2PO_2^- + H_2O + NiL_m^{2+} \rightarrow H_2PO_3^- + 2H^+ + Ni + mL \qquad (9)$$

Reaction (5) and (8) are combined:

$$3H_2PO_2^- + 2H^+ \rightarrow H_2PO_3^- + 2P + 3H_2O \qquad (10)$$

According to Reaction (9) and (10), 1 mol Ni deposition requires 1 mol $H_2PO_2^-$ and 1 mol P deposition requires 1.5 mol $H_2PO_2^-$. Reaction (7) is side reaction which makes no contribution to deposition and causes bath instability. The reduction efficiency is defined as consumption of hypophosphite for Ni and P deposition in a fixed time expressed as a percentage of hypophosphite consumed in the bath, as shown in Equation (3).

3.1.2 Plating rate equation

Plating rate equation can be expressed as follows [20]：

$$v = k\,[Ni^{2+}]^{0.67}[H_2PO_2^-]^{0.47}[L]^{-0.32}[H^+]^{-0.09}\exp\left(-\frac{E_a}{RT}\right) \qquad (11)$$

Equation (11) is applicable for $\rho(NiSO_4 \cdot 6H_2O)$ below 21.016 g·dm^{-3}. k is the pre-exponential factor of Arrhenius equation. E_a (J·mol^{-1}) is the apparent activation energy of Arrhenius equation. R (J·mol^{-1}·K^{-1}) is the gas constant. T (K) is the absolute temperature. [Ni^{2+}], [H$_2$PO$_2^-$], [L], [H$^+$] and [H$_2$PO$_3^-$] (g·dm^{-3}) refer to the concentration of the chemical species Ni^{2+}, H$_2$PO$_2^-$, L, H$^+$ and H$_2$PO$_3^-$, respectively.

By taking the logarithm of Equation (11), we obtain the following result:

$$\log v = \log k_1 + 0.67 \log[Ni^{2+}] + 0.47 \log[H_2PO_2^-] - 0.32 \log[L] + 0.09 pH - \frac{E_a}{2.303RT} \qquad (12)$$

3.2 Apparent activation energy of electroless Ni-P plating process

EN plating process required activation energy in order to trigger the reactions. This energy was supplied in the form of heat. The energy required by the system was one of the most important factors affecting the kinetics or rate of the deposion process. In order to study the effect of bath temperature, the amount of hypophosphite and nickel salt was conttolled at 25 g·dm^{-3} and 20 g·dm^{-3} respectively. Dependence of plating rate on temperature is shown in Curve A of Figure 1. Nickel ions did not deposit on magnesium substrate below 323 K. The plating rate was low and coatings were incompact in 333-353 K. Compact coatings were deposited at the plating rate above 10 μm·h^{-1} in 353-363 K. The bath stability was poor and even caused bath decomposition when bath temperature exceeded 363 K.
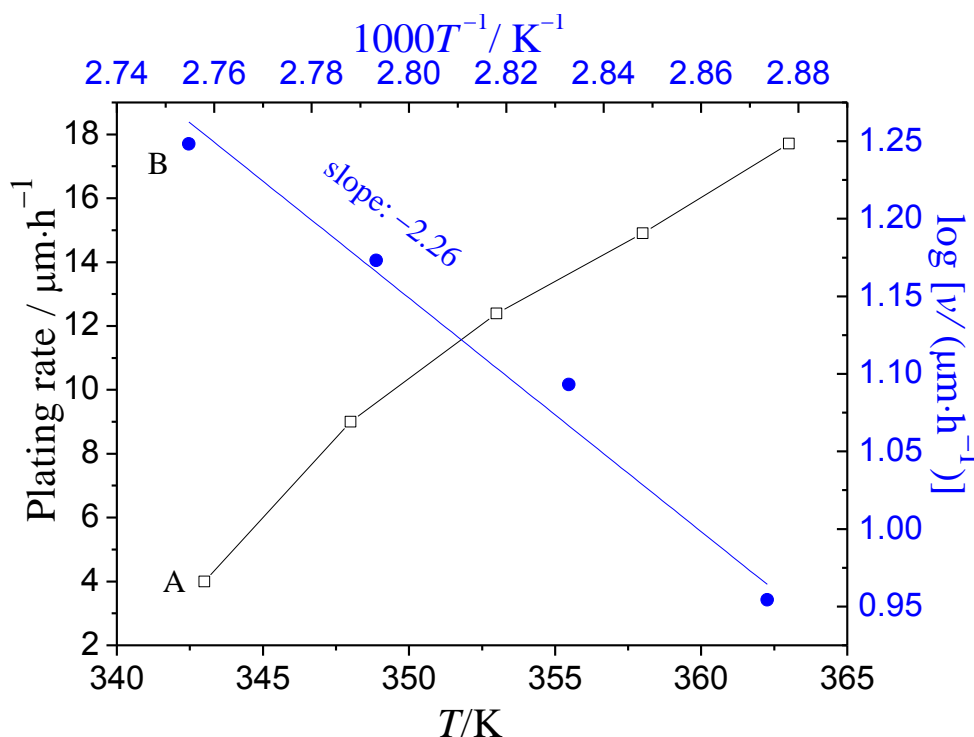

Figure 1. Dependence of plating rate on different temperature and the $\log v$-T^{-1} curves of EN deposition

Curve B of Figure 1 is the $\log v$-T^{-1} curves of EN deposition reaction. It exhibited the $\log v$ increased linearly with the reciprocal temperature in 353-363 K. According to Equation (12), according to the slope of the $\log v$-T^{-1} curves, the apparent activation energy can be calculated. It was 43.27 kJ·mol^{-1}, which was between 38-45 kJ·mol^{-1} obtained by other investigators [21, 22] from a similar EN condition. Based on the value of the apparent activation energy, the mechanism of electroless nickel plating should be chemically controlled.

3.3 Effect of sodium hypophosphite on bath reactivity and coatings qualities

3.3.1 Efficiency of nickel deposition, reducing efficiency and plating rate

Nickel salt was fixed at 20 g·dm^{-3} according to our previous study [10, 16] and bath temperature was controlled at 353 K based on Section 3.2. Effect of sodium hypophosphite on efficiency of nickel deposition (b), reducing efficiency (e_{SH}) and plating rate (v) are shown in Figure 2.
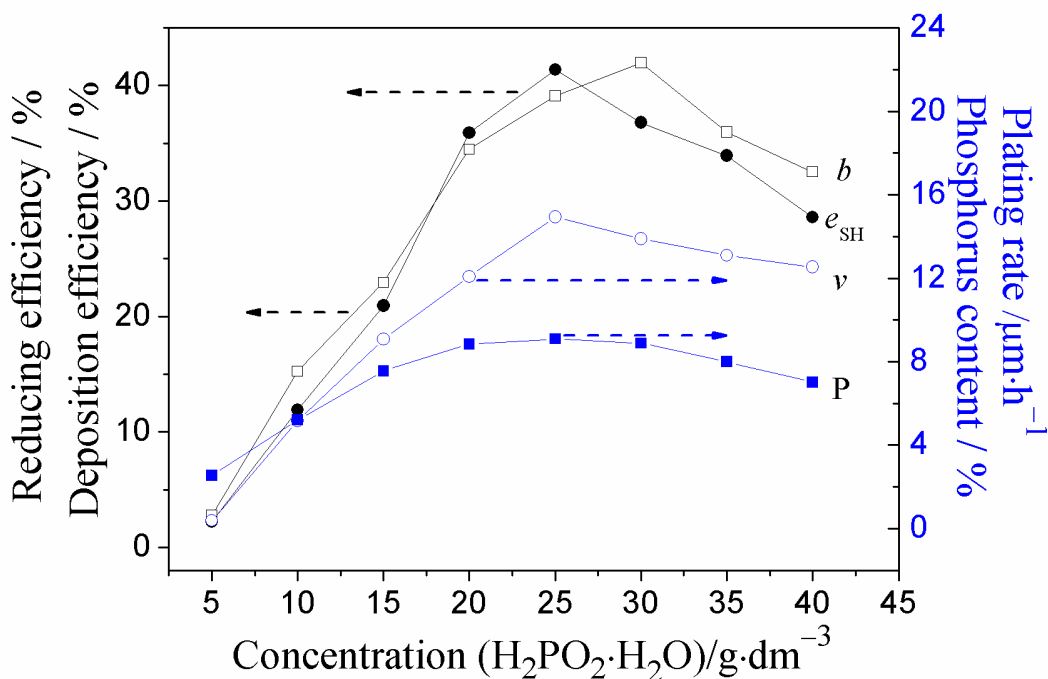
Figure 2. Dependence of deposition efficiency of nickel (b), reduction efficiency (e_{SH}), plating rate (v) and phosphorus content of coatings (P) on concentration of sodium hypophosphite

Efficiency of nickel deposition directly affected bath stability. Bath instability which even led to bath decomposition would cause massive discharge of waste and environmental pollution. The concentration of hypophosphite in the bath affected the bath activity and stability. Curve b in Figure 2 shows the dependence of efficiency of nickel deposition on sodium hypophosphite. The efficiency of nickel deposition increased with sodium hypophosphite increasing below 30 g·dm^{-3} NaH$_2$PO$_2$·H$_2$O in the bath. However, further increase of sodium hypophosphite led to decrease of the efficiency of nickel deposition beyond 30 g·dm^{-3} NaH$_2$PO$_2$·H$_2$O in the bath. This was attributed to the formation of

products of side reation during plating. The efficiency of nickel deposition reached 41.95 % when $NaH_2PO_2·H_2O$ in the bath equaled 25 $g·dm^{-3}$.

The change of Curve e_{SH} in Figure 2 was similar to Curve *b* in Figure 2, but reduction efficiency reached 41.36 % when $NaH_2PO_2·H_2O$ in the bath equaled 30 $g·dm^{-3}$. The difference of the above characteristic concentrations was produced because efficiency of nickel deposition neglected the side reaction (hydrogen evolution). Based on Curve *b* and e_{SH} in Figure 2, higher value of *b* and e_{SH} was obtained in 25-35 $g·dm^{-3}$ $NaH_2PO_2·H_2O$ in the bath.

The dependence of the plating rate on sodium hypophosphite is shown in Curve *v* of Figure 2. The plating rate increased with sodium hypophosphite increasing below 25 $g·dm^{-3}$ $NaH_2PO_2·H_2O$ in the bath. It was consistent with the Equation (11). If sodium hypophosphite further increased beyond 25 $g·dm^{-3}$ $NaH_2PO_2·H_2O$ in the bath, it led to the decrease of the plating rate because proportion of side reaction was increased and diffusion and adsorption of hypophosphite were enhanced. Concerning plating rate, appropriate range of $NaH_2PO_2·H_2O$ in the bath should be controlled in 25-35 $g·dm^{-3}$.

3.3.2 Phosphorus content in Ni-P coatings

Phosphorus of coatings was derived from hypophosphite reactions. The concentration of hypophosphite directly influenced the phosphorus content in coatings.

The phosphorus content in coatings with sodium hypophosphite is shown in Curve P in Figure 2. The phosphorus content in coatings with sodium hypophosphite could be illustrated based on the following empirical kinetic equation [5]:

$$\frac{d[P]}{dt} = k\left[H_2PO_2^-\right]^{1.91}\left[H^+\right]^{0.25}$$

(13)

The phosphorus content in coatings increased with sodium hypophosphite increasing below 25 $g·dm^{-3}$ $NaH_2PO_2·H_2O$ in the bath. This was consistent with Equation (13). However, phosphorus content in coatings decreased beyond 25 $g·dm^{-3}$ $NaH_2PO_2·H_2O$ in the bath. It was attributed to intensification of hypophosphite diffusion and adsorption as well as the increase of the proportion of hydrogen evolution. The Ni-P coatings with above 8 wt.% phosphorus content formed amorphous alloy structure with good corrosion resistance [23] in the bath containing 18-30 $g·dm^{-3}$ $NaH_2PO_2·H_2O$. The phosphorus content of coatings could be controlled by adding different concentration of sodium hypophosphite in the bath and adjusting bath pH.

3.3.3 pH variation

Reaction (4) generated 1 mol H^+ when consumed 4 mol $H_2PO_2^-$ in the process of EN plating. The H^+ increase in the plating solution would depressed the pH value of the bath. The pH value of bath was changed with various concentration of sodium hypophosphite during electroless plating. Dependence of the bath pH after electroless plating on sodium hypophosphite is shown in Figure 3. The pH value of bath after electroless plating was the lowest in the bath containing 25 $g·dm^{-3}$ $NaH_2PO_2·H_2O$. It was attributed to the reatively low proportion of hydrogen evolution and the

reatively high proportion of Reaction (6) and (8), which was consistent with Curve e_{SH} in Figure 2. The concentration of hypophosphite influenced the bath pH, as well as changed the performance of bath and coatings. According to our previous studies and literature data [24], adding ammonium acetate could maintain pH stable in the bath.
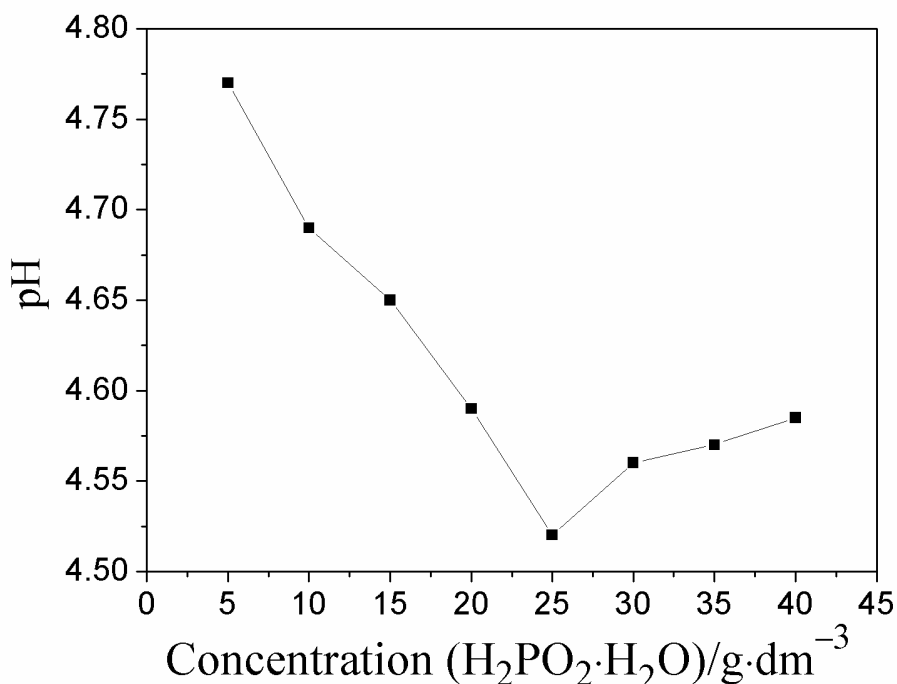
Figure 3. Dependence of the bath pH after electroless plating on concentration of sodium hypophosphite

3.4 Coatings qualities

3.4.1 Coverage and adhesion of coatings

**Table 2.** Dependence of the coatings coverage and adhesion on sodium hypophosphite

Concentration of sodium hypophosphite (g·dm^{-3})	Corrosion spots (cm^{-2})	Adhesion
5	0.4	×
10	0.15	×
15	0.1	Δ
20	0	○
25	0	○
30	0	○
35	0	○
40	0	×

Note: "×" stands for very poor adhesion and plating continuously sloughed-off;
"Δ"indicates sometimes small plating swell occurs but no peeling off;
"○" represents good qualities plating without swell and peel off.

The dependence of coverage and adhesion of coatings on sodium hypophosphite is shown in Table 2. In the bath containing 20-35 $g\cdot dm^{-3}$ $NaH_2PO_2\cdot H_2O$, no corrosion spots in coatings formed and the coatings possessed good adhesion after operation of section 2.3(4). It was because of appropriate plating rate and efficiency of nickel deposition could made nickel ions deposit uniformly on magnesium substrate.

3.4.2 Corrosion resistance

According to the discussion in Section 3.2.2, appropriate range of $NaH_2PO_2\cdot H_2O$ in the bath should be controlled in 20-30 $g\cdot dm^{-3}$. Polarization curves of the coatings obtained from the bath containing 20, 25 and 30 $g\cdot dm^{-3}$ $NaH_2PO_2\cdot H_2O$ is shown in Figure 4. The corrosion potential (E_{corr}), corrosion current density (i_{corr}) and Tafel slopes (b_a and b_c) of Curve A, Curve B and Curve C from Figure 4 are shown in Table 3. The corrosion potentials of the coatings obtained were basically close in the bath containing 20, 25 and 30 $g\cdot dm^{-3}$ $NaH_2PO_2\cdot H_2O$. But the corrosion current density of the coatings formed in the bath containing 30 $g\cdot dm^{-3}$ $NaH_2PO_2\cdot H_2O$ was the lowest. The lower corrosion current density, the higher corrosion resistant of coatings [25, 26].
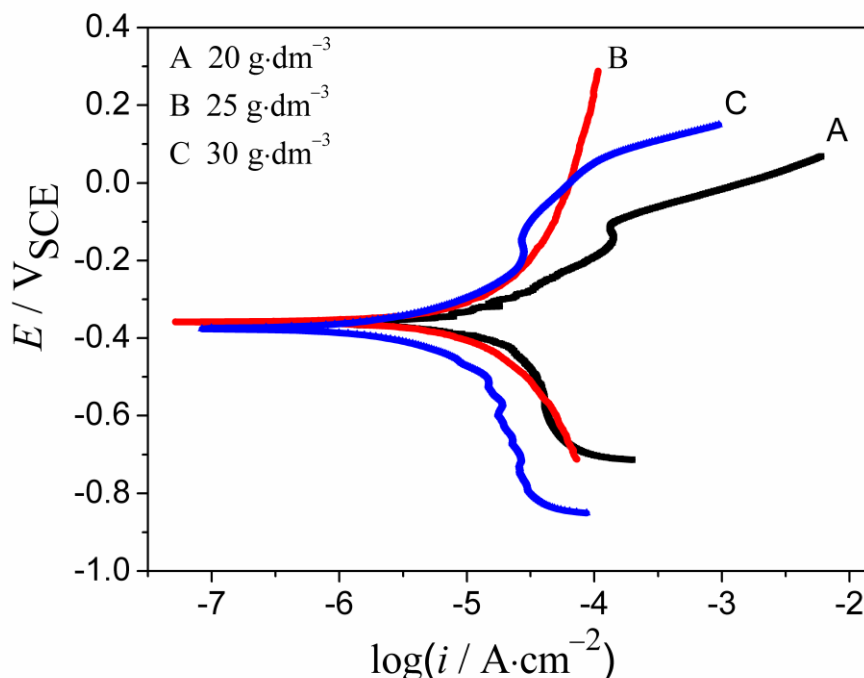

Figure 4. Polarization curves of the coatings obtained in the bath containing 20, 25 and 30 $g\cdot dm^{-3}$ $NaH_2PO_2\cdot H_2O$

Figure 5(A) shows the SEM images of morphology of coatings in the bath containing 25 $g\cdot dm^{-3}$ $NaH_2PO_2\cdot H_2O$ after electroless plating before 96 h NSS test. No corrosion spots appeared in the coatings. Some pinholes on the coating obtained in the bath containing 25 $g\cdot dm^{-3}$ $NaH_2PO_2\cdot H_2O$ after

96 h NSS were observed in Figure 5(B). The pinholes on the Ni-P coatings were produced since of hydrogen bubbles were evolved during EN plating. They were not corrosion points because black points around the holes were not seen.

Table 3. The corrosion potential (E_{corr}), corrosion current density (i_{corr}) and the Tafel slopes (b_a and b_c) of Curve A, Curve B and Curve C in Figure 4.

	E_{corr} /V	i_{corr} /A·cm^{-2}	b_a /V	b_c /V
Curve A	−0.3645	1.862×10^{-5}	0.34692	0.6716
Curve B	−0.3612	1.100×10^{-5}	0.31822	0.3508
Curve C	−0.3739	7.056×10^{-6}	0.25747	0.3879
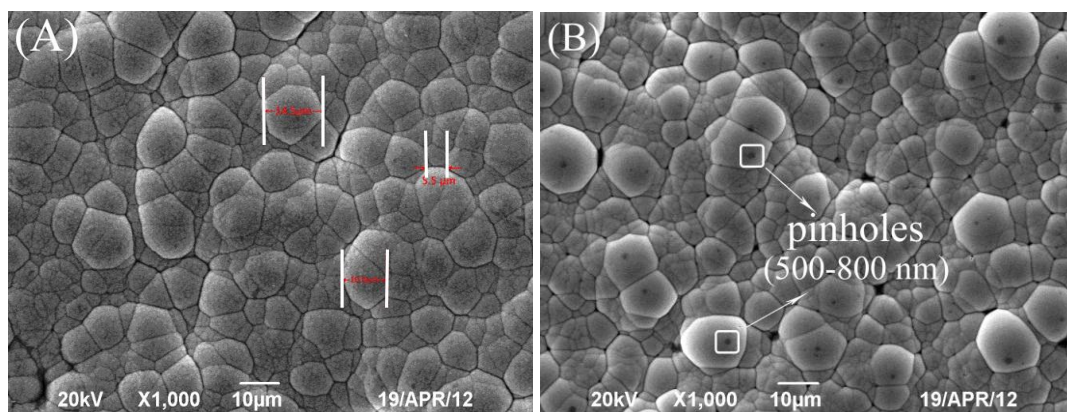
Figure 5. SEM images of morphology of coatings in the bath containing 25 g·dm^{-3} NaH$_2$PO$_2$·H$_2$O before and after 96 h NSS test

No corrosion spots in the coatings were observed after 96 h NSS test in the bath containing 20, 25 and 30 g·dm^{-3} NaH$_2$PO$_2$·H$_2$O.

4. CONCLUSIONS

(1) The optimum quantity of NaH$_2$PO$_2$·H$_2$O used in the bath can obviously improve the efficiency of nickel deposition, reduction efficiency and the bath life. The compact Ni-P coatings with high adhesion and good corrosion resistance were easily obtained. The effect of concentration of sodium hypophosphite provided a route for controlling properties of coatings and monitoring bath stability.

(2) Reduction product H$^+$ had influence on the plating. pH could be maintained stable via adding ammonium acetate.

(3) The apparent activation energy was required during EN deposition reaction. Elevation of temperature could accelerate the Ni-P deposition reaction. When the bath temperature was controlled to 353-363 K, electroless Ni-P plating conducted fluently.

References

1. S. Ranganatha, T.V. Venkatesha, K. Vathsala, *Appl. Surf. Sci.*, 256 (2010) 7377.
2. M. Novak, D. Vojtech, T. Vıtub, *Appl.Surf. Sci.*, 256 (2010) 2956.
3. S.M. Abd El Halleml, I. Ghayad, M. Eisaa, N. Nassif, M.A.Shoeib, H. Soliman, *Int. J. Electrochem. Sci.*, 9 (2014) 2005-2015.
4. X.C. Wang, W.B. Cai, W.J. Wang, H.T. Liu, Z.Z. Yu, *Surf. Coat. Technol.*, 168 (2003) 300.
5. Z.Z. Qiu, R. Wang, X. H. Wu, Y.S. Zhang, *Int. J. Electrochem. Sci.*, 8 (2013) 195 -1965.
6. G.O. Mallory, J.B. Hajdu, *Electroless Plating: Fundamentals and Applications*, American, Electroplaters and Surface Finishers Society, Orlando (1990).
7. J.T. Winowlin Jappes, B. Ramamoorthy, P. Kesavan Nair, *J. Mater. Process. Technol.*, 169 (2005) 308.
8. M. Anık, E. Körpe, *Surf. Coat. Technol.*, 201 (2007) 4702.
9. J.Z. Li, Z.C. Shao, X. Zhang, *Surf. Coat. Technol.*, 200 (2006) 3010.
10. H.L. Wang, L.Y. Liu, W.F. Jiang, *Adv. Mater. Res.*, 418-420 (2012) 936.
11. Z.H. Xie, G. Yu, B.N. Hu, X.P. Lei, T.J. Li, J. Zhang , *Appl. Surf. Sci.*, 257 (2011) 5025.
12. W.J. Cheong, B.L. Luan, D.W. Shoesmith, *Appl. Surf. Sci.*, 229 (2004) 282.
13. E.I. Ryabinina, N.V. Sotskaya, K.S. Shikhaliev, *Russ. J. Appl. Chem.*, 72 (1999) 1932.
14. J.S. Li, *Plat. Environmental.*, 22 (2002) 17.
15. W.X. Zhang, J.G. He, Z.H. Jiang, Q. Jiang, J.S. Lian, *Surf. Coat. Technol.*, 201 (2007) 4594.
16. J.L. Chen, G. Yu, B.N. Hu, Z. Liu, L.Y. Ye, Z.F. Wang, *Surf. Coat. Technol.*, 201 (2006) 686.
17. ISO 3768-1976, *Metallic coatings - Neutral salt spray test (NSS test)*, USA (1990).
18. H. Ashassi-Sorkhabi, A. Mirmohseni, H. Harrafi, *Electrochimi. Acta,* 50 (2005) 5526.
19. G.F. Cui, N. Li, D.Y. Li, J. Zheng, Q.L. Wu, *Surf. Coat. Technol.,* 200 (2006) 6808.
20. Z.H. Xie, G. Yu, T.J. Li, Z.J. Wu, B.N. Hu, *J. Coat. Technol. Res.,* 9 (2012) 107.
21. A.P. Ordine, S.L. Díaz, I.C.P. Margarit, O.E. Barcia, O.R. Mattos, *Electrochimi. Acta,* 51 (2006) 1480.
22. B.N. Hu, R.X. Sun, G. Yu, L.S. Liu, Z.H. Xie, X.M. He, X.Y. Zhang, *Surf. Coat. Technol.,* 228 (2013) 84.
23. Z.H. Xie, G. Yu, B.N. Hu, X.Y. Zhang, L.B. Li, W.G. Wang, D.C. Zhang, *Int. J. Electrochem. Sci.,* 8 (2013) 6664.
24. M.Y. Abyaneh, A. Sterritt, T.J. Mason, *J. Electrochem. Soc.,* 154 (2007) D467.
25. Y.W. Song, D.Y. Shan, E.H. Han, *Electrochimi. Acta,* 53 (2007) 2009.
26. S. Amira, D. Dubé, R. Tremblay, E. Ghali, *Mater. Charact.,* 59 (2008) 1508.